

Feature Selection and Estimation of Route and Gait During Walking With Route and Speed Changes by Surface Electromyograph Using Transformer

Naoki Nozawa¹, Yusuke Osawa¹, and Keiichi Watanuki^{1,2}

¹Graduate School of Science and Engineering, Saitama University, 255 Shimo-okubo, Sakura-ku, Saitama-shi, Saitama 338–8570 Japan

²Advanced Institute of Innovative Technology, Saitama University, 255 Shimo-okubo, Sakura-ku, Saitama-shi, Saitama 338–8570 Japan

ABSTRACT

In recent years, several gait support and training devices have been developed to improve the walking ability of the elderly. However, most of these devices are only intended for straight walking on flat surfaces and do not support turning or acceleration/deceleration. This study investigated the possibility of predicting velocity changes using surface EMG (sEMG) and machine learning methods. The ultimate goal was to develop walking aids and training devices that can help with turning and acceleration/deceleration movements. The R² score of the true value and the predicted value was 0.630 ± 0.107 , indicating moderate accuracy, and the trend of the time series was successfully captured. It is possible to predict the velocity from the sEMG potentials of the Medial Hamstrings and Medial Head of Gastrocnemius through feature selection.

Keywords: Gait analysis, Unsteady walking, Machine learning, Transformer

INTRODUCTION

In recent years, researchers have developed various gait support and training devices to improve the walking ability of the elderly. However, most of these devices are designed for straight walking on flat surfaces and do not support unsteady walking such as turning, acceleration/deceleration, and ascending/descending stairs. Unsteady walking accounts for 40% of daily walking (Brain et al., 2007), highlighting the need for the development of gait support and training devices that can support unsteady walking. To support unsteady movements, the system must predict the user's condition and provide support based on the predicted values. This study investigated the possibility of predicting speed changes during wayfinding walking using surface electromyography (sEMG). Wayfinding walking is a common activity in which individuals walk in search of a destination in a given area. It involves various unsteady elements such as turning and acceleration/deceleration. To make predictions, a machine learning model has been developed that uses a Transformer structure that has proven successful in fields such as natural language processing and computer vision.

Muscle Activity and Gait Acquisition Experiments During Walking

As part of the study, experiments were conducted to measure muscle activity and gait during walking.

Equipment Used and Test Muscles

A wireless electromyograph, motion capture system, and destination indication system were used for the experiment. The wireless electromyograph had a sampling frequency of 1,000 Hz. Ten electromyographs were attached on each side of the five test muscles that exhibited significant myoelectric paths during turning.

- Tensor Fasciae Lates (TFL)
- Vastus Medialis Oblique (VMO)
- Medial Hamstrings (MH)
- Medial Head of Gastrocnemius (MHG)
- Tibialis Anterior (TA)

The muscles were positioned as follows: for the TFL, on the muscle belly of the two transverse fingers anteriorly inferior to the superior anterior iliac spine; for the VMO, on the muscle belly of the two transverse fingers proximal to the bottom of the patella and inclined inwards at an angle of approximately 55° to the long femoral axis. The MH electrode was placed on the muscle belly approximately 15 cm proximal to the patellar cleft, the MHG electrode was placed on the muscle belly five transverse fingers distal to the knee socket skin line. The TA electrode was placed on the muscle belly on the medial side of the tibial ridge distal to the four transverse fingers from the tibial rough surface. The electrodes were placed on the left and right legs in a targeted manner.

The destination is indicated along the subject's walking route via LEDs as part of the destination indication system. The LEDs were controlled by a Raspberry Pi and remotely controlled via SSH communication. During the exploratory walk, participants randomly selected illuminated LEDs as their destinations. All devices were connected to a single PC and time-synchronized, as shown in Figure 1.

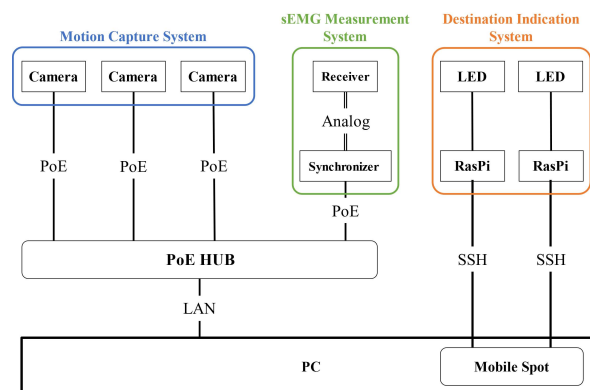


Figure 1: Communication system for experimental devices.

Experimental Environment and Walking Route

The experiment was conducted in an indoor room that was at least 3 m high, 5 m wide, and 20 m deep, and was free of furniture. Eight cameras were positioned to cover an area 3 m high and 12 m wide, as shown in Figure 2. Six LEDs were placed around the shooting area as landmarks for exploratory walking. Three walking paths were created for the experiment: straight ahead along the diagonal line of the shooting range, as shown in Figure 3a; clockwise and counterclockwise around the walking path, as shown in Figure 3b; and in the direction of the LEDs illuminated by the destination indication system, as shown in Figure 3c.

Experimental Procedure

The experiment was conducted with a male participant (22 years old) with the approval of the Human Ethics Committee of Saitama University. Electromyographs and markers were attached to the participant’s test muscles before they were asked to wear a motion-capture suit. The participant completed the walking task in 27 trials, performing three trials at three different speeds (subjective normal speed, subjective high speed, and subjective slow speed) on both straight and circular routes. The participant then completed five trials of the walking task using the destination indication system on the wayfinding route.

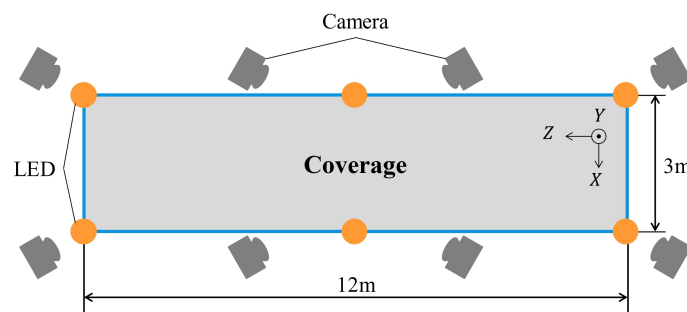


Figure 2: Experimental environment.

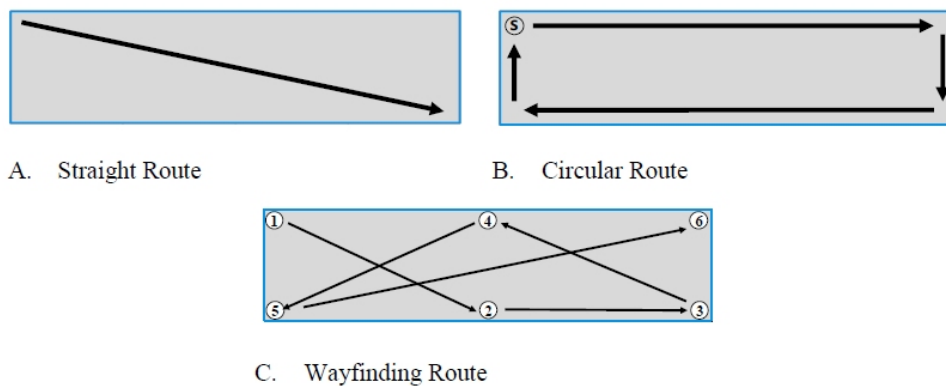


Figure 3: Walking route.

Data Processing for the Construction of Velocity Prediction Models

The following process was applied to the sEMG and motion-capture data acquired during the experiment.

Noise Reduction and Normalization of sEMG

To remove power supply and body motion noise in the sEMG, a Butterworth bandpass filter with passing frequencies in the range of 20–450 Hz was applied based on the work of De Luca et al. The data distribution was then smoothed using the root mean square of the moving average (MoveRMS) expressed in equation (1) and adjusted using the Box-Cox transform from equation (2) (see Figure 4).

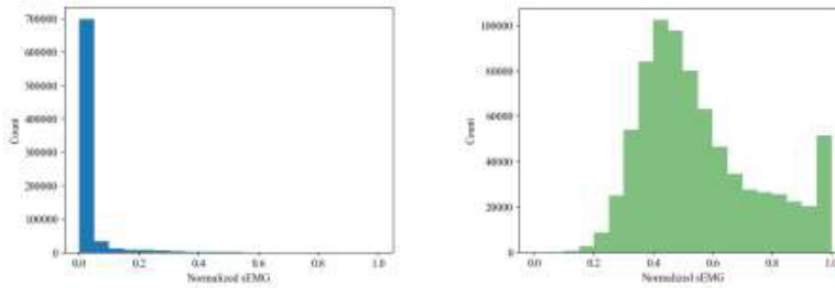
$$\text{MoveRMS}(x_i) = \sqrt{\frac{1}{N} \sum_{j=i}^{i+N-1} (x_j^2)} \quad (1)$$

$$\text{BoxCox}(x, \lambda) = \begin{cases} \frac{x^\lambda - 1}{\lambda}, & \lambda \neq 0 \\ \log(x), & \lambda = 0 \end{cases} \quad (2)$$

Lambda (λ) was calculated using maximum likelihood estimation. The value of λ that maximizes the log-likelihood function $L(\lambda)$ expressed in equation (3) was used. Normalization was then performed using the maximum (x_{\max}) and minimum values (x_{\min}), as expressed in equation (4), to ensure that the data fell between 0 and 1.

$$L(\lambda) = (\lambda - 1) \sum_i (\log(x_i)) - \frac{N}{2} \log \left(\frac{\sum_i (x_i^{(\lambda)} - x^{(\lambda)})^2}{N} \right) \quad (3)$$

$$\text{Normalize}(x) = \frac{x - x_{\min}}{x_{\max} - x_{\min}} \quad (4)$$



A. Distribution before the transformation

B. Distribution after the transformation

Figure 4: Changes in sEMG data distribution due to Box-Cox transformation.

Calculation and Normalization of the Straight-Line Directional Velocity

The data obtained from the motion capture contained missing values owing to shielding and other factors; therefore, a second-order spline interpolation

was performed. The center of gravity G in the absolute coordinate system XYZ was then determined using the coordinates of the four markers RA , LA , RP and LP attached to the waist, as shown in Figure 5, with reference to the origin of the captured area. The reference vector R was determined as described in equation (5).

$$R = LA - RA = (R_x, R_y, R_z) \quad (5)$$

The experiment was conducted on a floor without undulations. Therefore, it was assumed that there was no change in the height direction, and the velocity change in the XZ plane was analyzed. The reference vector and the center of gravity at time t were labelled as R_t and G_t , respectively. The relative coordinate system $X'Z'$ was used, with the X' axis parallel to R_t . The velocity v_t was determined by taking the time derivative of the center of gravity coordinates, $G_{t+1} - G_t$. Equation (6) shows how it can be converted into a relative coordinate system using the rotation matrix $R(-\theta)$.

$$v'_t = R(-\theta_t) v_t = \begin{bmatrix} \cos \theta_t & \sin \theta_t \\ -\sin \theta_t & \cos \theta_t \end{bmatrix} \begin{bmatrix} v_{t,x} \\ v_{t,z} \end{bmatrix} \quad (6)$$

The Z' component of the velocity v'_t expressed in the relative coordinate system is defined as the Straight-Line Directional Velocity. Similar to the sEMG, the velocity was normalized using the maximum and minimum values to ensure that the data ranged between zero and one.

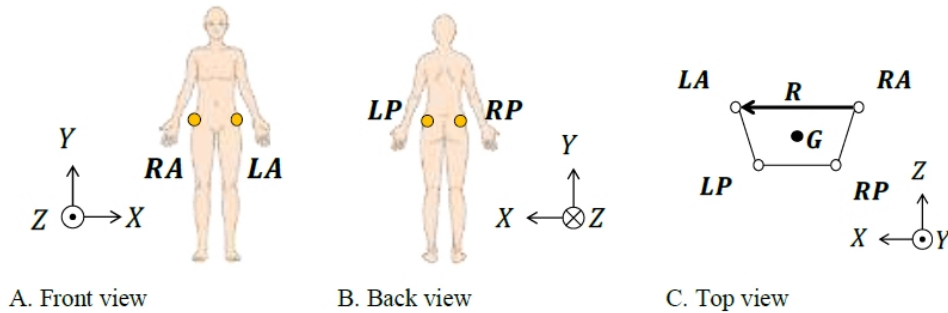


Figure 5: Marker mounting position and coordinates.

Creating Datasets With Lag Features

Let $X = \{X_1, X_2, \dots, X_n \mid X_i \in \mathbb{R}^{10}\}$ be the processed sEMG time series and $Y = \{Y_1, Y_2, \dots, Y_n \mid Y_i \in \mathbb{R}^1\}$ be the Straight-Line Directional Velocity time series, where X_t and Y_t represent the states at time t . If lag features are used to predict the next l datasets from the past k datasets, the datasets can be expressed as shown in equations (7) and (8):

$$X_t^{(k)} = \{X_{t-k}, X_{t-k+1}, \dots, X_{t-1} \mid X_i \in \mathbb{R}^{10}\} \quad (7)$$

$$Y_t^{(l)} = \{Y_t, Y_{t+1}, \dots, Y_{t+l-1} \mid Y_i \in \mathbb{R}^1\} \quad (8)$$

Building a Model to Predict Straight-Line Directional Velocity

A prediction model with a Transformer encoder (Vaswani et al., 2017), as shown in Figure 7a, was created to predict the straight-line directional velocity from the previous sEMGs. The model consists of four layers of Transformer encoders, each of which contains a Multi Head attention and a feedforward network (FFN), with residual learning applied through a skip connection (Figure 7b).

Multi Head attention and five attention mechanisms were arranged in parallel to extract different representations (Figure 7c). In this architecture, self-attention can capture the relationship between different parts of each input, and attention is computed using equation (9), whereas FFN uses GELU, represented by equation (10), as the activation function to achieve non-linear transformation and random regularization (Hendrycks and Gimpel, 2016), where Φ represents the standard normal distribution function.

During training, one trial of the five wayfinding walks was used as test data to evaluate the performance of the model, while 90 % of the remaining data were used for training the model, and 10 % were used to validate overfitting (Figure 8). The datasets for each of the five wayfinding walking trials were designated as Fold 1 to Fold 5, and the model was evaluated by cross-validation. The relevant parameters for training were the mean absolute error (MAE) as the loss function, Adam as the optimization algorithm, a learning rate of 0.001, a batch size of 16, and 50 epochs.

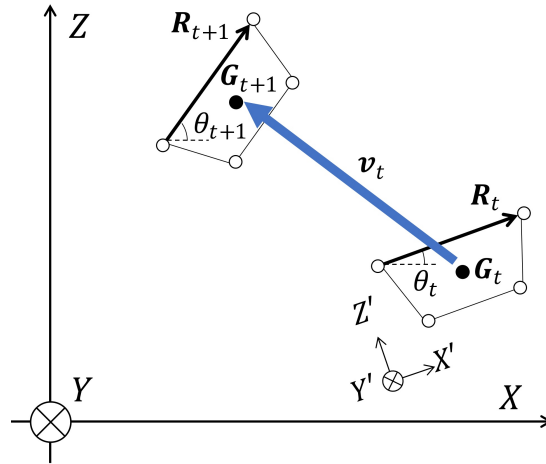


Figure 6: Straight-line directional velocity at time t .

$$\text{Attention}(\mathbf{Q}, \mathbf{K}, \mathbf{V}) = \text{softmax}\left(\frac{\mathbf{Q} \cdot \mathbf{K}^T}{\sqrt{d_k}}\right) \mathbf{V} \quad (9)$$

$$\text{GELU}(x) = x \cdot \Phi(x) \quad (10)$$

$$\text{FFN}(x) = \mathbf{W}_1 \cdot \text{GELU}(\mathbf{W}_0 x + \mathbf{b}_0) + \mathbf{b}_1 \quad (11)$$

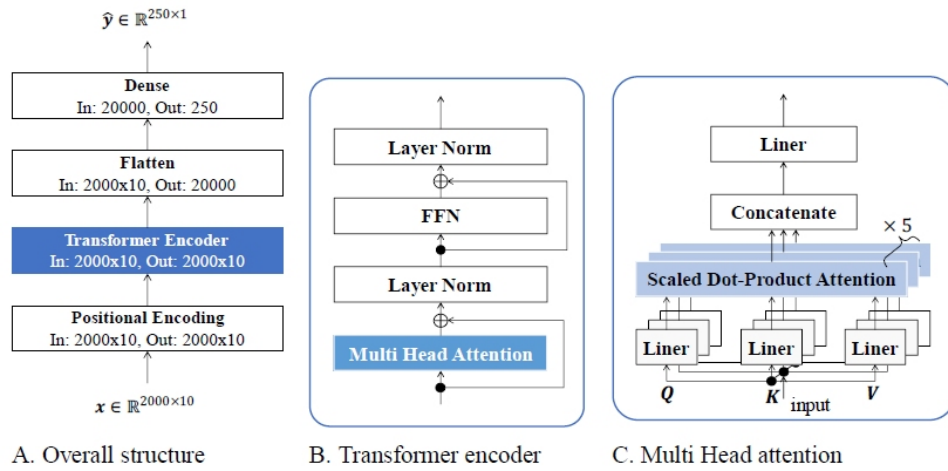


Figure 7: Constructed straight-line directional velocity prediction model.

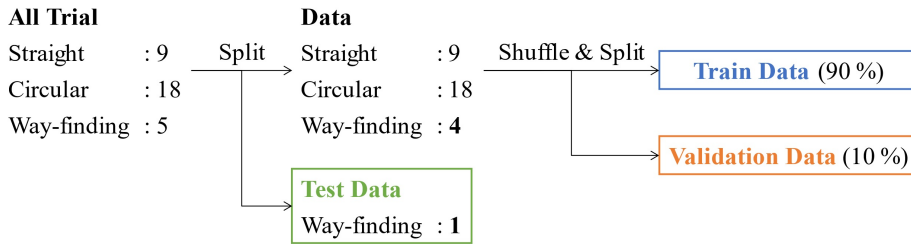


Figure 8: Data splitting procedure.

Evaluation of Predicted Results

Table 1 lists the evaluation indices for each Fold. Figure 9 shows the true and predicted values for Fold 5. Although the trend of the time series was well captured, some output values differed from the true values. Figure 10 illustrates the permutation feature importance (PFI), which indicates the importance of the features.

Table 1. Prediction results for each fold.

Fold	MAE	RMSE	R2
1	0.080	0.110	0.699
2	0.081	0.107	0.717
3	0.092	0.117	0.690
4	0.090	0.119	0.576
5	0.094	0.124	0.466
Total	0.087±0.006	0.115±0.007	0.630±0.107

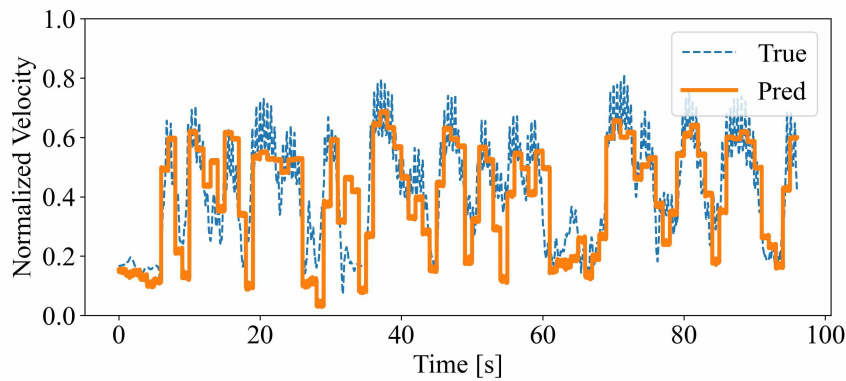


Figure 9: True and predicted values of the test data in fold 5.

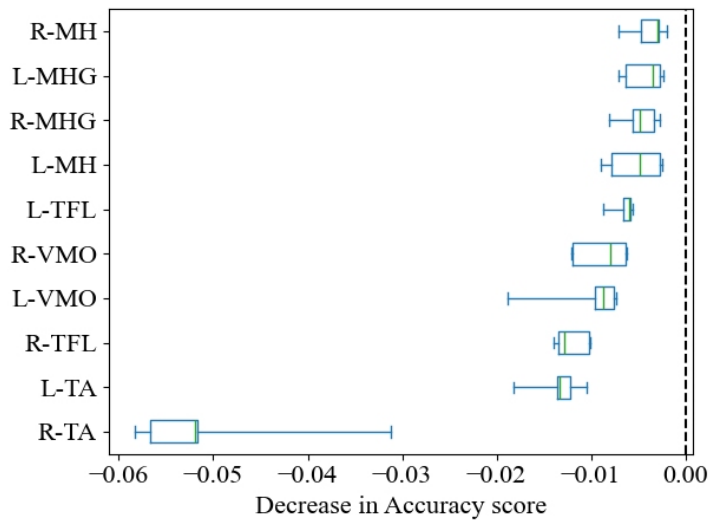


Figure 10: PFI score for the training data.

CONSIDERATION

The PFI score showed that the MH and MHG were significant features. Therefore, training was conducted using only the MH and MHG sEMGs as input. The results are listed in Table 2. Although the accuracy decreased, some predictions were possible. Walking speed can be predicted from sEMG of the MH and MHG muscles alone. The MH is a muscle group that performs extension of the knee joint and extension and adduction of the hip joint, and it is hypothesized that prediction of these movements from the sEMG predicts the straight-line directional velocity during walking.

It is hypothesized that the larger error observed when only some sEMGs are used as input is related to the swaying motion during walking. During human gait, the body sways from side to side to maintain balance, and this swaying cannot be predicted by MH and MHG alone. To reduce the error, it is considered effective to remove the noise caused by swaying from the

straight-line velocity or select muscles to predict swaying and use them for training.

CONCLUSION

The aim of this study was to develop a system to support and train non-stationary walking and to investigate whether it is possible to predict straight-line directional velocity using the sEMG. The distribution of the sEMG data was adjusted using a Box-Cox transformation, and the straight-line velocity was calculated using a rotation matrix. With this data, a dataset was created, and a machine learning model was trained. The results showed that changes in velocity during the exploration walk were adequately captured. The results also suggest that the sEMG of the medial hamstrings and medial head of the gastrocnemius may be able to predict velocity changes.

Table 2. Prediction results using only the MH and MHG sEMGs for each epoch.

Fold	MAE	RMSE	R2
1	0.130	0.166	0.311
2	0.143	0.178	0.216
3	0.145	0.187	0.206
4	0.129	0.179	0.042
5	0.159	0.192	-0.270
Total	0.141±0.012	0.180±0.010	0.101±0.229

REFERENCES

- Brain, G. C., Greta, B. C, Glenn, K. K., and Micheal, S. O. (2007). “Video task analysis of turning during activities of daily living”, *Gait & Posture*, Volume 25 No. 2, pp. 289–294. <https://doi.org/10.1016/j.gaitpost.2006.04.003>
- De Luca, C. J., Gilmore, L. D., Kuznetsov, M., and Roy, S. H. (2010). “Filtering the surface EMG signal: Movement artifact and baseline noise contamination”, *J Biomech*, Volume 43 No. 8, pp. 1573–1579. <https://doi.org/10.1016/j.jbiomech.2010.01.027>
- Hendrycks, D., and Gimpel. K. (2016). “Gaussian Error Linear Units (GELUs)”, [online]. [Preprint]. [Viewed 13 August 2024]. Available from: <https://arxiv.org/abs/1606.08415>
- Vaswani, A., Shazeer, N., Parmar, N., Uszkoreit, J., Jones, L., Gomez, N. A., Kaiser, L., and Polosukhin, I. (2017). “Attention is All You Need”, *Adv Neural Inf Process Syst*, Volume 30.